Endogenous p53 expression in human and mouse is not regulated by its 3′UTR

Sibylle Mitschka and Christine Mayr*

Cancer Biology and Genetics Program, Memorial Sloan Kettering Cancer Center, New York, NY 10065, USA

*Correspondence: mayrc@mskcc.org

Christine Mayr
Memorial Sloan Kettering Cancer Center
1275 York Ave, Box 303
New York, NY 10065
Phone: 646-888-3115

Abstract

Inactivation of p53 occurs in many cancers. microRNAs and RNA-binding proteins are thought to repress p53 expression through its 3′ untranslated region (3′UTR), thus contributing to tumorigenesis. We used CRISPR/Cas9 to delete the human and mouse p53 3′UTRs while preserving endogenous mRNA processing. This revealed that the endogenous 3′UTR is not involved in the regulation of p53 mRNA or protein expression, neither in steady state nor after genotoxic stress.

Main

The transcription factor p53 coordinates the cellular stress response. p53 regulates expression of genes involved in cell cycle control, DNA repair, apoptosis, metabolism, and cell differentiation [1]. Reduced levels or insufficient p53 activity are major risk factors for the development of cancer, whereas hyperactive p53 has been linked to impaired wound healing, obesity and accelerated aging [2]. Posttranslational modifications of p53 together with cofactor recruitment regulate the activity of p53 and MDM2 is the major regulator of p53 protein abundance [3].

Another widely studied element of p53 expression regulation is the 3′UTR of the *TP53* mRNA which contains binding sites for microRNAs (miRNAs), lncRNAs, and RNA-binding proteins [4]. A large number of reporter assays demonstrated the repressive nature of the *TP53* 3′UTR. These

studies suggested that miRNAs and RNA-binding proteins prevent p53 hyperactivation under normal conditions and induce p53 protein translation after exposure to genotoxic stress [5-7].

Here, we generated mice and engineered human cell lines using CRISPR/Cas9 to delete the *TP53* and *Trp53* 3′UTRs at orthologous human and mouse gene loci while keeping mRNA processing intact. In HCT116 cells and in mouse tissues, we did not observe 3′UTR-dependent differences in mRNA or p53 protein levels under normal conditions or after induction of DNA damage. When using the *TP53* 3′UTR in isolation, we confirmed the previously observed repressive effects in reporter assays. Adding the p53 coding region to the reporters had a substantially stronger repressive effect on expression that was not further enhanced by the 3′UTR. Reporter assays that investigate *TP53* 3′UTR elements in isolation seem to overestimate its repressive effects as the endogenous human and mouse 3′UTRs do not contribute to the regulation of p53 expression.

The generation of mature mRNAs requires the polyadenylation signal and surrounding sequence elements that recruit mRNA 3′ end processing factors. These factors mostly bind within 150 nucleotides upstream of the cleavage site [8], thus making this part of the 3′UTR essential. Human and mouse mRNAs contain substantially longer 3′UTRs than strictly necessary for 3′ end processing. The additional sequence enables regulatory functions through miRNAs and RNA-binding proteins which mostly bind to the upstream non-essential part of 3′UTRs [9].

Here, we used zygotic injection of a pair of CRISPR/Cas9 guide RNAs to delete the non-essential part of the mouse *Trp53* 3′UTR (Fig. 1a, blue) to investigate its contribution to p53 expression regulation. Mice with a homozygous deletion of the 3′UTR, called ΔUTR (dUTR), were viable, fertile, and did not show any development defects (Supplementary Fig. 1). We measured *Trp53* mRNA expression in ten different tissues and did not detect significant differences between wild-type (WT) and dUTR samples (Fig. 1b). DNA damage induces p53 protein expression through higher translation rates and lower protein turnover [10]. To examine the role of the 3′UTR in the regulation of stimulus-dependent p53 expression, we performed total body irradiation of WT and dUTR mice. At four hours post-irradiation, p53 protein expression levels were upregulated to a similar extent in spleen, liver, and colon samples from WT and dUTR mice (Fig. 1c).

A highly dosage-sensitive p53 target gene is *Cdkn1a* that encodes the cell cycle regulator p21 [11]. Four hours after irradiation, *Cdkn1a* mRNA levels were similarly induced in WT and dUTR mice, suggesting that p53 target gene activation is 3′UTR-independent in mouse tissues (Fig.

1d). These results indicate that the non-essential part of the *Trp53* 3′UTR is not required for steady-state or stimulus-dependent regulation of p53 mRNA or protein levels in mice.

Most of the work that established a role for the 3′UTR as a regulator of p53 expression was performed in human cell lines (Supplementary Table 1). To investigate the role of the endogenous human *TP53* 3′UTR we used CRISPR/Cas9 to delete the 3′UTR in HEK293 cells and in the human colon carcinoma cell line HCT116, an established model for investigating p53-dependent functions. The 3′UTR deletion removed 1,048 nucleotides, corresponding to 88% of the 3′UTR in WT cells. The deletion affected almost all previously reported binding sites for regulatory miRNAs, lncRNAs, and RNA-binding proteins, while preserving 3′ end processing (Fig. 2a and Supplementary Fig. 2a, 2b).

In both cell lines and in several clones obtained from HCT116 cells with a homozygous deletion of the *TP53* 3′UTR, we did not observe differences in p53 mRNA and protein expression levels in steady state cultivation conditions (Fig. 2b, 2c and Supplementary Fig. 2c, 2d). To assess stimulus-dependent p53 expression, we generated genotoxic stress using the topoisomerase inhibitor etoposide. The kinetics and dosage dependency of p53 expression was similar in WT and dUTR cells (Fig. 2d, 2e). A 3′UTR-independent p53 induction was also observed with additional stress stimuli, including Nutlin-3, an inhibitor of MDM2, treatment with 5-fluorouracil, a thymidylate synthase inhibitor, or UV irradiation (Fig. 2f).

Most previous studies that investigated 3′UTR-dependent regulation of p53 abundance used reporter genes as proxy for endogenous p53 regulation (Supplementary Table 1). We cloned the human *TP53* 3′UTR or the dUTR fragment downstream of GFP and expressed the constructs in p53-/- HCT116 cells (Fig. 2g and Supplementary Fig. 2e-g). In the context of the reporter, the *TP53* 3′UTR reduced expression of both GFP mRNA and protein several fold (Fig. 2g). This result was recapitulated when using luciferase instead of GFP reporters, thus confirming previous findings (Supplementary Fig. 2h). When we included the *TP53* coding region without the p53 3′UTR in the GFP reporter, we observed a 20-fold reduction in mRNA and a five-fold reduction in protein levels (Fig. 2g). Importantly, addition of the *TP53* 3′UTR in the context of the coding region did not further repress mRNA and protein expression of the GFP reporter and abrogated the difference between the samples containing the dUTR and full-length 3′UTR (Fig. 2g).

Our results indicate that the different parts of mRNAs do not act autonomously, but are part of a regulatory unit and functionally cooperate with each other [7,12]. Our observations support the recently established role of the coding region as major regulator of mRNA stability and

translation [13,14]. Although our data indicate that p53 abundance regulation is 3′UTR-independent, the human p53 3′UTR may still have important functions possibly through control of protein localization or protein activity as has been shown for other proteins [9,15-17].

Our data further suggest that repressive effects on p53 that were previously attributed to 3′UTR-dependent abundance regulation may be indirect as many miRNAs and RNA-binding proteins target several members of the p53 network [7,18-20]. Our study shows that genetic manipulation of endogenous 3′UTRs may be an important tool to disentangle direct from indirect post-transcriptional effects. It should become an essential step during the testing of miRNA-based therapies that are being explored as anti-cancer therapeutics in the context of p53 to avoid mixed or negative results in large clinical trials [21-23].

Acknowledgements

We thank all members of the Mayr lab for helpful discussions and critical reading of the manuscript. We thank the Mouse Genetics Core Facility at MSKCC for assistance in the generation of Trp53 dUTR mice. This work was funded by a postdoctoral fellowship from the DFG to S.M. and by the NIH Director's Pioneer Award (DP1-GM123454), the Pershing Square Sohn Cancer Research Alliance to C.M., and the NCI Cancer Center Support Grant (P30 CA008748).

Author contributions

S.M. performed all experiments and analyses. S.M. and C.M. conceived the project, designed the experiments, and wrote the manuscript.

Declaration of Interests

The authors declare no competing interests.

Figure legends

Figure 1. Knockout of the *Trp53* 3′UTR does not lead to aberrant p53 expression in a mouse model.

a, Schematic of the mouse *Trp53* gene. The sequence deleted in dUTR cells is shown in blue.

b, *Trp53* mRNA in tissues from WT and dUTR mice was normalized to *Gapdh*. Shown is mean + s.d. from n=3 independent experiments.

c, Representative immunoblots of p53 protein from tissues obtained from three mice four hours after total body irradiation. Gy, Gray.

d, *Cdkn1a* mRNA expression of samples from **(c)** was normalized to *Gapdh*. Shown is mean + s.d. from three mice.

Figure 2. 3′UTR-independent p53 expression regulation in human cells in steady state or after stress.

a, Schematic of the human *TP53* gene. The sequence deleted in dUTR cells is shown in blue. Tracks of binding sites for miRNAs, RBPs and lncRNA are depicted below (see also Supplementary Table 1).

b, *TP53* mRNA expression levels in WT HCT116 cells and three different dUTR cell clones are shown from n=3 independent experiments (mean + s.d.) after normalization to *GAPDH*.

c, As in **b**, but shown is p53 protein expression. Actin serves as loading control.

d, Immunoblot showing p53 protein levels after four hours of etoposide (Eto) treatment (0-32 μM) in WT and dUTR HCT116 cells. GAPDH serves as loading control.

e, As in **d**, but cells were treated with 0.5 μM etoposide for 0, 24 and 48 hours. Actin serves as loading control.

f, As in **d**, but cells were treated with 20 μM etoposide, 40 μM 5-fluorouridine (5-FU), 20 μM Nutlin-3 or 50 J/m^2 UV. Actin serves as loading control.

g, GFP protein levels were quantified by FACS and *GFP* mRNA levels were measured by RT-qPCR using *GAPDH* as housekeeping gene in p53 -/- HCT116 cells. Shown is mean + s.d. of n=3 independent experiments. CDS, coding sequence. T-test for independent samples was performed, * p<0.05, ** p<0.01, *** p<0.0001; ns, not significant.

Supplementary Figure 1. Generation and characterization of *Trp53* dUTR mice.

a, Schematic of the mouse *Trp53* gene. The sequence deleted in dUTR cells is shown in blue and binding sites of primers used for PCR screening are marked with arrows.

b, Screening PCR of mice that were born after zygotic injection of CRISPR/Cas9 ribonucleoprotein particles targeting the *Trp53* 3′UTR. The predicted lengths of the PCR products from WT and dUTR alleles are indicated. Mice that were selected for validation by sequencing are labeled in red.
c, Sequence alignments of *Trp53* dUTR alleles of select founder mice shown in **b**. Male mice #3 and #26 harboring identical DNA deletions were used to establish a mouse colony.
d, Genotypes of pups from 28 *Trp53* dUTR heterozygous intercrosses. Unknown refers to mice that died before weening.
e, Weights of mice at 10-11 weeks of age are shown for WT, *Trp53* dUTR heterozygous and homozygous males. Data are shown as mean + s.d. with n=6 in each group.

Supplementary Figure 2. Generation and characterization of *TP53* dUTR human cell lines.
a, Sequence alignment of *TP53* alleles spanning the deletion in WT and dUTR HEK293 and HCT116 cell clones analyzed in this study. Binding sites of guide RNAs (gRNAs) used to produce the deletion are underlined in the WT reference sequence and predicted cutting sites are marked by a scissor symbol.
b, Northern blot analysis of *TP53* mRNA from WT and dUTR HEK293 cells. A probe that hybridizes to the *TP53* coding region (CDS) reveals expression of a shortened *TP53* mRNA in dUTR cells. The size difference is consistent with the length of the CRISPR-mediated deletion. A probe designed to bind the *TP53* 3′UTR does not produce a signal in the mRNA of dUTR cells, confirming removal of this sequence element. The band of 18S rRNA is used as a loading control. * indicates an unspecific band from ribosomal rRNA.
c, Analysis *TP53* mRNA levels in WT, protein knockout (KO), and dUTR HEK293 cells was measured by RT-qPCR and normalized with *GAPDH* mRNA levels. Shown are mean + s.d. of n=7 independent experiments.
d, Immunoblot showing p53 protein level in HEK293 cells, grown under steady-state conditions.
e, As in **d**, but shown are HCT116 cells.
f, Gating strategy in FACS experiment for measurement of GFP protein expression in cells.
g, Histogram plots from one representative FACS experiment from Fig. 2g. The grey area represents the untransfected GFP-negative control population.
h, Renilla luciferase activity of constructs containing either the human dUTR or the human full-length *TP53* 3′UTR was measured in p53 -/- HCT116 cells. Shown is mean + s.d. of n=3 independent experiments after normalization to firefly luciferase. t-test for independent samples, * $p<0.05$.

References

1 Kastenhuber, E. R. & Lowe, S. W. Putting p53 in Context. *Cell* **170**, 1062-1078 (2017).

2 Rufini, A., Tucci, P., Celardo, I. & Melino, G. Senescence and aging: the critical roles of p53. *Oncogene* **32**, 5129-5143 (2013).

3 Hafner, A., Bulyk, M. L., Jambhekar, A. & Lahav, G. The multiple mechanisms that regulate p53 activity and cell fate. *Nature reviews. Molecular cell biology* **20**, 199-210 (2019).

4 Haronikova, L., Olivares-Illana, V., Wang, L., Karakostis, K., Chen, S. & Fahraeus, R. The p53 mRNA: an integral part of the cellular stress response. *Nucleic Acids Res* **47**, 3257-3271 (2019).

5 Fu, L. & Benchimol, S. Participation of the human p53 3'UTR in translational repression and activation following gamma-irradiation. *EMBO J* **16**, 4117-4125 (1997).

6 Mazan-Mamczarz, K., Galban, S., Lopez de Silanes, I., Martindale, J. L., Atasoy, U., Keene, J. D. & Gorospe, M. RNA-binding protein HuR enhances p53 translation in response to ultraviolet light irradiation. *Proc Natl Acad Sci U S A* **100**, 8354-8359 (2003).

7 Zhang, J., Cho, S. J., Shu, L., Yan, W., Guerrero, T., Kent, M., Skorupski, K., Chen, H. & Chen, X. Translational repression of p53 by RNPC1, a p53 target overexpressed in lymphomas. *Genes Dev* **25**, 1528-1543 (2011).

8 Martin, G., Gruber, A. R., Keller, W. & Zavolan, M. Genome-wide analysis of pre-mRNA 3' end processing reveals a decisive role of human cleavage factor I in the regulation of 3' UTR length. *Cell reports* **1**, 753-763 (2012).

9 Mayr, C. What Are 3' UTRs Doing? *Cold Spring Harb Perspect Biol* **11** (2019).

10 Kumari, R., Kohli, S. & Das, S. p53 regulation upon genotoxic stress: intricacies and complexities. *Molecular & cellular oncology* **1**, e969653 (2014).

11 Fischer, M. Conservation and divergence of the p53 gene regulatory network between mice and humans. *Oncogene* **38**, 4095-4109 (2019).

12 Theil, K., Imami, K. & Rajewsky, N. Identification of proteins and miRNAs that specifically bind an mRNA in vivo. *Nature communications* **10**, 4205 (2019).

13 Wu, Q., Medina, S. G., Kushawah, G., DeVore, M. L., Castellano, L. A., Hand, J. M., Wright, M. & Bazzini, A. A. Translation affects mRNA stability in a codon-dependent manner in human cells. *eLife* **8** (2019).

14 Narula, A., Ellis, J., Taliaferro, J. M. & Rissland, O. S. Coding regions affect mRNA stability in human cells. *RNA* **25**, 1751-1764 (2019).

15 Berkovits, B. D. & Mayr, C. Alternative 3' UTRs act as scaffolds to regulate membrane protein localization. *Nature* **522**, 363-367 (2015).

16 Lee, S. H. & Mayr, C. Gain of Additional BIRC3 Protein Functions through 3'-UTR-Mediated Protein Complex Formation. *Mol Cell* **74**, 701-712 e709 (2019).

17 Kwon, B., Patel, N.D., Lee, S.H., Lee, J., Ma, W., Mayr, C. . Enhancers regulate polyadenylation site cleavage and control 3′UTR isoform expression. *bioRxiv*, doi: https://doi.org/10.1101/2020.1108.1117.254193 (2020).

18 Shu, L., Yan, W. & Chen, X. RNPC1, an RNA-binding protein and a target of the p53 family, is required for maintaining the stability of the basal and stress-induced p21 transcript. *Genes Dev* **20**, 2961-2972 (2006).

19 Le, M. T. *et al.* Conserved regulation of p53 network dosage by microRNA-125b occurs through evolving miRNA-target gene pairs. *PLoS Genet* **7**, e1002242 (2011).

20 Zhang, M., Xu, E., Zhang, J. & Chen, X. PPM1D phosphatase, a target of p53 and RBM38 RNA-binding protein, inhibits p53 mRNA translation via dephosphorylation of RBM38. *Oncogene* **34**, 5900-5911 (2015).

21 Kasinski, A. L. & Slack, F. J. Epigenetics and genetics. MicroRNAs en route to the clinic: progress in validating and targeting microRNAs for cancer therapy. *Nat Rev Cancer* **11**, 849-864 (2011).

22 Hermeking, H. MicroRNAs in the p53 network: micromanagement of tumour suppression. *Nat Rev Cancer* **12**, 613-626 (2012).

23 Bonneau, E., Neveu, B., Kostantin, E., Tsongalis, G. J. & De Guire, V. How close are miRNAs from clinical practice? A perspective on the diagnostic and therapeutic market. *Ejifcc* **30**, 114-127 (2019).

Mitschka, Figure 1

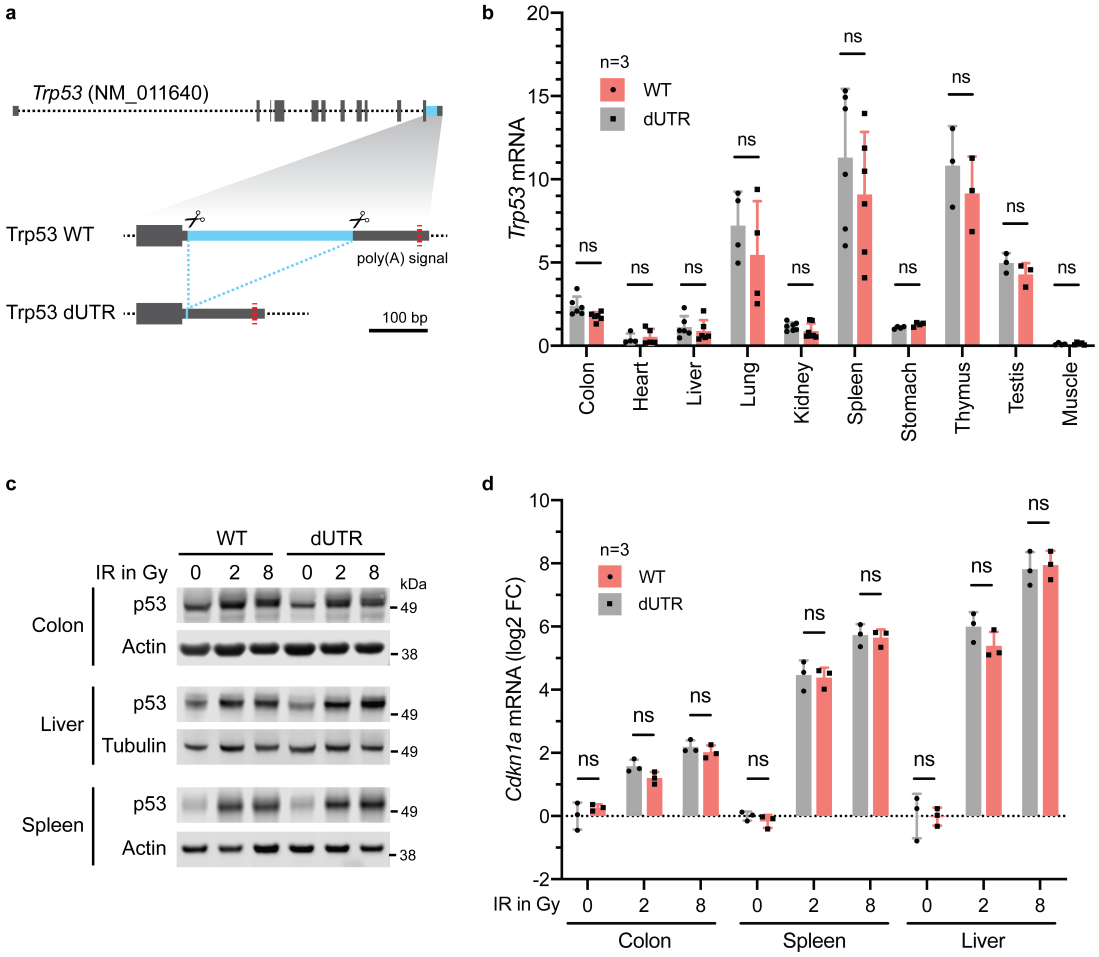

Mitschka, Figure 2

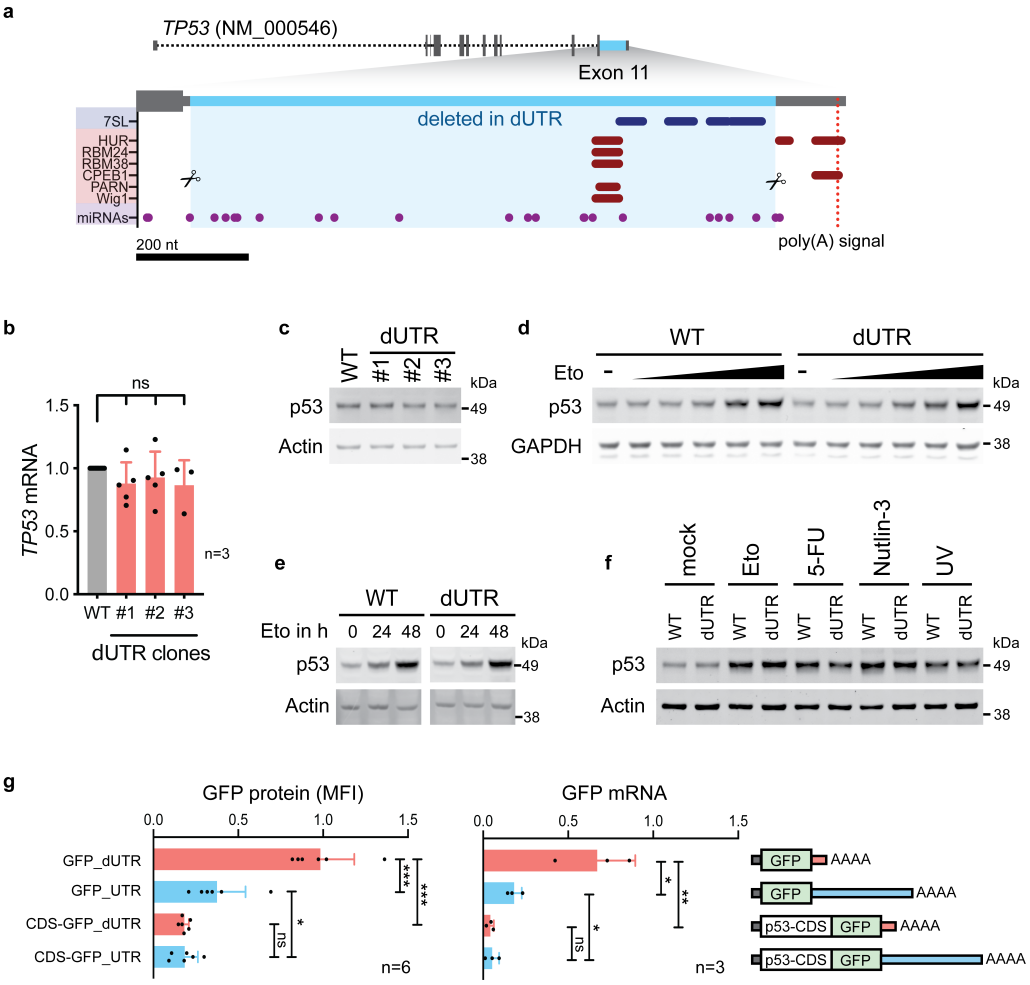

Supplementary Table 1. Previously reported evidence of miRNAs, lncRNAs, and RNA-binding proteins that target the p53 3'UTR.

Interactors of the human *TP53* mRNA mapping to the last exon					
Name	**Type**	**Binding region (NM_000546.6)**	**Affected in dUTR allele?**	**Experiments**	**References (PMID)**
miR-1228-3p	miRNA	1422-1428	yes	LRA, RT-qPCR, IHC, WB	25422913
miR-125a-5p	miRNA	2044-2063	yes	LRA, NB, RT-qPCR, WB	19818772
miR-125b-5p	miRNA	2043-2064	yes	LRA, ISH, RT-qPCR, WB	19293287, 21935352, 27592685
miR-1285-3p	miRNA	2113-2134	yes	LRA, RT-qPCR, WB	20417621
miR-150-5p	miRNA	1568-1580	yes	LRA, WB	23747308
miR-151a-5p	miRNA	2304-2325	yes	LRA, ChIP-seq, RT-qPCR, WB	27191259
miR-200a-3p	miRNA	2269-2291	yes	LRA, WB	23144891
miR-24-3p	miRNA	2352-2374	yes	LRA, IHC, RT-qPCR, WB	27780140
miR-25-3p	miRNA	1401-1423	yes	LRA, RT-qPCR, WB	20935678
miR-30d-5p	miRNA	1596-1618	yes	LRA, RT-qPCR, WB	20935678
miR-375	miRNA	1462-1483	yes	LRA, Flow, RT-qPCR, WB, IF	23835407
miR-663a	miRNA	1260-1281	no (in CDS)	LRA	27105517
miR-504	miRNA	2059-2066, 2387-2395	yes, no	LRA, RT-qPCR, WB	20542001
miR-92	miRNA	1417-1422	yes	LRA, WB	21112562
miR-141	miRNA	2285-2290	yes	LRA, WB	21112562
miR-638	miRNA	1381-1404	yes	LRA, WB, IP	25088422
miR-3151	miRNA	1337-1354	yes	LRA, WB, RT-qPCR	24736457
miR-33	miRNA	1957-1980	yes	LRA, WB	20703086
miR-380-5p	miRNA	1909-1936, 1943-1974	yes, yes	LRA, WB	20871609
miR-19b	miRNA	1712-1734	yes	LRA, WB	24742936
miR-15a	miRNA	2394-2414	no	LRA, WB	21205967
miR-16	miRNA	2394-2415	no	LRA, WB	21205967
miR-584	miRNA	1263-1284	no (in CDS)	LRA, WB, IP	25088422
WIG1	RBP	2064-2106	yes	LRA, IP, RT-qPCR	19805223
PARN	RBP	2071-2102	yes	LRA, EMSA, IP, RT-qPCR	23401530
CPEB1	RBP	2458-2500	no	IP, RT-PCR	19141477
RBM38 (RNPC1)	RBP	2064-2106	yes	EMSA, IP, RT-PCR, Polysome gradient	21764855, 24142875, 25823026
RBM24	RBP	2064-2106	yes	LRA, EMSA, IP, RT-qPCR,	29358667
HUR	RBP	2064-2106, 2393-2412, 2458-2505	yes, yes, no	LRA, EMSA, WB, RT-qPCR	12821781, 14517280, 16690610, 18680106
7SL	lncRNA	2107-2149, 2194-2240, 2269-2301, 2307-2362	yes, yes, yes, yes	LRA, IP, WB	25123665

Interactors of the murine *Trp53* mRNA mapping to the last exon					
Name	**Type**	**Binding region (NM_011640.3)**	**Affected in dUTR allele?**	**Experiments**	**References (PMID)**
miR-92a-3p	miRNA	1646-1666	yes	LRA, WB	22451425
Tia1	RBP	1426-1442, 1702-1731	yes, no	LRA, iCLIP	28904350
Hzf	RBP	1345-1395, 1529-1574	yes, yes	LRA, EMSA, WB, IP, RT-qPCR, Polysome gradient	21402775

Abbreviations: LRA: luciferase reporter assay; WB: western blot; IP: co-immunoprecipitation assay; RT-qPCR: quantitative reverse transcription PCR; NB: northern blot; IHC: immunohistochemistry; ISH: In situ hybridization; EMSA: electromobility shift assay.

Mitschka, Supplementary Figure 1

a

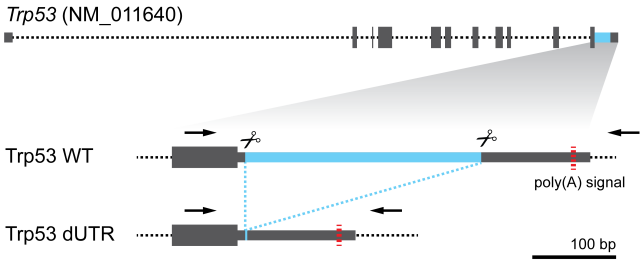

b

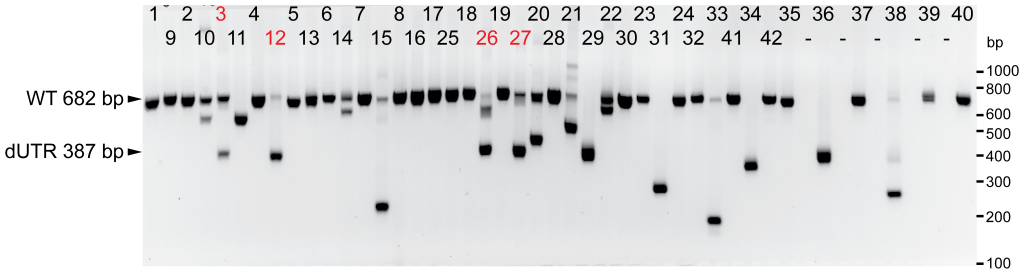

c

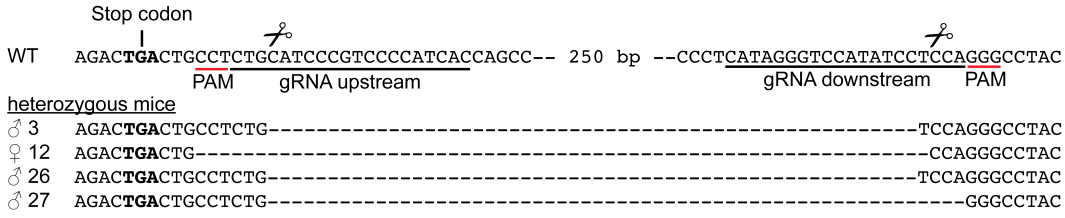

d

Het ♂ x Het ♀ (28 litters)	n	% of total	% expected
Total	162	100	100
Wildtype	35	21.6	25
Heterozygous	81	50	50
Homozygous	36	22.2	25
Unknown[1)]	9	5.6	0

e

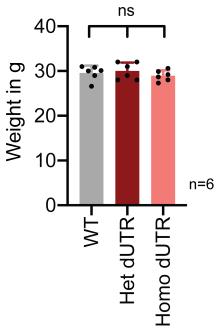

Mitschka, Supplementary Figure 2

a

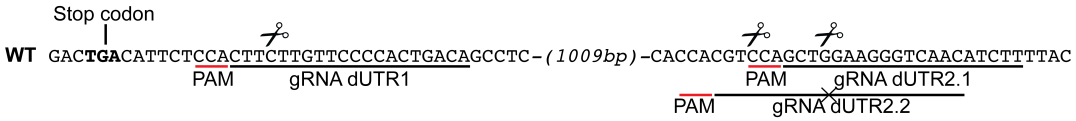

TP53 dUTR HEK293

```
1   GACTGACAT----------------------------------------------------------GGTCAACATCTTTTAC
2   GACTGACATTCTCCACTTC------------------------------------------GGAAGGGTCAACATCTTTTAC
```

TP53 dUTR HCT116#1

```
1   GACTGACATTCTCCACTTC--------------------------------------CAGCT-GAAGGGTCAACATCTTTTAC
2   GACTGACATTCTCCACTTCTTGTTCCCCACTG-----------------------------GAA----CAACATCTTTTAC
```

TP53 dUTR HCT116#2

```
1   GACTGACATTCTCCACTTCTTGTTCCCCACTG-----------------------------GAA----CAACATCTTTTAC
2   GACTGACATTCTCCACTTCTTGTTCCCCACTG-------------------------------AAGGGTCAACATCTTTTAC
```

TP53 dUTR HCT116#3

```
1   GACTGACATTCTCCACTT------------------------------------------GGAAGGGTCAACATCTTTTAC
2   GACTGACATTCTCCACTTC-----------------------------------------GGAAGGGTCAACATCTTTTAC
```

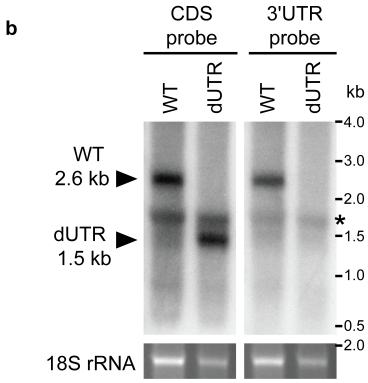

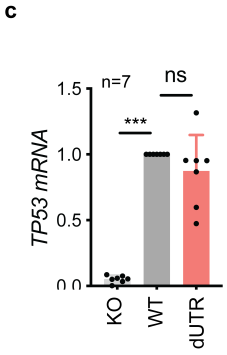

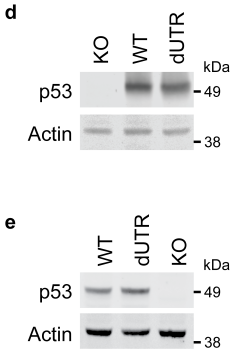

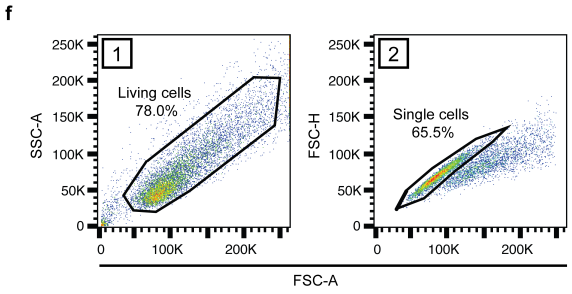

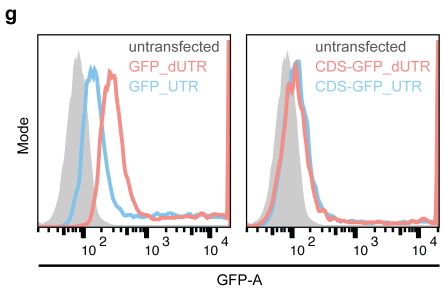

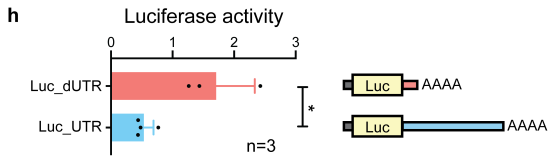

Methods

Generation of the *Trp53* dUTR mouse strain using CRISPR/Cas9

Female C57Bl/6 mice between 3-4 weeks of age were superovulated by intraperitoneal injection of Gestyl followed by human chorionic gonadotropin according to standard procedures [1]. After superovulation, the females were setup with male studs for mating. After mating, fertilized eggs were recovered at the one-cell stage from oviducts of superovulated female mice. 1-2 pl of CRISPR/Cas9 RNP complexes were injected into the pronuclei of fertilized eggs (see details below). Surviving eggs were surgically reimplanted into the oviducts of pseudo-pregnant females previously primed for pregnancy by mating with vasectomized males. The resulting pubs were screened using PCR for the deletion amplicon at two weeks of age (primers are listed in Table S2). Suitable candidates were further validated by sequencing.

Preparation of CRISPR-Cas9 RNP injection mixture. Two target-specific crRNAs and a tracrRNA were purchased from IDT (Table S2). In two separate tubes, 2.5 µg of each crRNA was mixed with 5 µg tracrRNA, heated to 95 °C for 5 min and then slowly cooled down to room temperature for annealing. The annealed duplexes were combined and mixed with 1 µg recombinant Cas9 enzyme (PNABIO) and 625 ng *in vitro* transcribed Cas9 mRNA and the total volume was adjusted to 50 µl with sterile water.

Screening for homozygous and heterozygous dUTR mice. Two heterozygous founder males with an identical 295 nucleotide deletion (Figure S1c) were used to establish a mouse colony. Two or more rounds of backcrossing into wildtype C57Bl/6 mice were performed prior to analysis of *Trp53* dUTR mouse phenotypes. Mouse genotypes from tail biopsies were determined using RT-PCR with specific probes designed for each Trp53 allele (Transnetyx, Cordova, TN).

Irradiation of mice. Where indicated, adult mice underwent total body irradiation with 2 or 8 Gy using a Cs-137 source in a Gammacell 40 Exactor (MDS Nordion) at 77 cGy/min. Four hours later, irradiated mice were euthanized to collect samples. All procedures were approved by the Institutional Animal Care and Use Committee at MSKCC under protocol 18-07-010.

Extraction of total RNA from mouse tissues and human cells for RT-qPCR analysis

For RNA extraction from mouse tissue, freshly collected tissue samples were flash frozen and transferred to RNAlater-ICE Frozen Tissue Transition Solution (Invitrogen). After soaking

overnight at -20 °C, the tissue samples were homogenized in vials containing 1.4 mm ceramic beads (Fisherbrand) and 400 µl RLT buffer (Qiagen) using a bead mill (Bead Ruptor 24, Biotage). 200 µl of the tissue homogenate was mixed with 1 ml of TRI Reagent (Invitrogen). For extraction of RNA from cultured cells, the cell pellet was directly resuspended in TRI Reagent. Total RNA extraction was performed according to the manufacturer's protocol. The resulting RNA was treated with 2U DNaseI enzyme (NEB) for 30 min at 37 °C, followed by acidic phenol extraction and isopropanol precipitation. To generate cDNA, about 200 ng of RNA was used in a reverse transcription reaction with SuperScript IV VILO Master Mix (Invitrogen). To measure the relative expression levels of mRNAs by RT-qPCR, FastStart Universal SYBR Green Master (ROX) from Roche was used together with gene-specific primers listed in Table S2. GAPDH/Gapdh was used as reference gene.

Generation of the *TP53* 3′UTR deletion in HCT116 and HEK293 cells

To generate CRISPR/Cas9 constructs, we annealed target-specific gRNA sequences and inserted them into a BbsI-digested pX330-U6-Chimeric_BB-CBh-hSpCAs9 vector (Addgene plasmid #42230) [2,3]. 1 µg of each pX330-gRNA plasmid plus 0.1 µg of pmaxGFP plasmid (Lonza) were transiently transfected into exponentially growing cells using Lipofectamine 2000 (Invitrogen). Three days after transfection, single GFP-positive cells were sorted into 96-well plates and cultured until colonies formed. The genomic DNA from individual cell clones was extracted using QuickExtract DNA Extraction Solution (Lucigen) and screened by PCR for the deletion amplicon using the DNA primers listed in Table S2. In the case of HCT116 cells, we repeated the above-described process using two different heterozygous clones with a new downstream gRNA to obtain homozygous *TP53* dUTR cells. Finally, to validate positive cell clones, all *TP53* alleles of candidate clones were sequenced (Figure S2d).

Generation of p53 KO HCT116 and HEK293 cells

We generated our own p53-deficient HEK293 and HCT116 cell lines by targeting exon 6 of the p53 coding region with a gRNA causing frame shift mutations. Specifically, pX330 plasmid harboring a p53-specific gRNA (Table S2) was transfected into HEK293 and HCT116 cells using Lipofectamine 2000 (Invitrogen). Two days later, the cells were split and seeded sparsely on a 10 cm dish in the presence of 10 µM Nutlin-3 (Seleckchem) which was used to select

against growth of p53-competent cells. After ten days, single colonies were picked, and individual clones were validated by WB for loss of p53 expression.

Western blot analysis

RIPA buffer (10 mM Tris-HCL pH 7.5, 150 mM NaCl, 0.5 mM EDTA, 0.1% SDS, 1% Triton X-100, 1% deoxycholate, Halt Protease Inhibitor Cocktail (Thermo Scientific)) was used to extract total protein from cultured cells or mouse tissues. Cell pellets were washed with PBS and directly resuspended in lysis buffer and incubated on ice for 30 min. Mouse tissue samples were homogenized in RIPA buffer using a bead mill in vials filled with 1.4 mm ceramic beads. Tissue lysates were sonicated to shear genomic DNA prior to removing insoluble components by centrifugation (10 min, 15,000 g). The proteins in the supernatant were precipitated by adding 0.11 volumes of ice-cold 100 % Trichloroacetic acid (TCA) and incubated at -20C for one hour. The samples were centrifuged (10 min, 15,000 g) and the pellet was washed twice in ice-cold acetone before resuspending in reducing 2x Laemmli buffer (Alfa Aesar). Proteins were separated by size on a 4-12% Bis-Tris SDS-PAGE gels (Invitrogen) and blotted on a 0.2 µm nitrocellulose membrane (BIO-RAD). The membrane was then incubated with primary antibody in Odyssey Blocking buffer (LI-COR) overnight at 4 °C. The following primary antibodies were used in this study: anti-human p53 (Santa Cruz, sc-47698, mouse, 1:250), anti-mouse p53 (Cell Signaling, #2524, mouse, 1:500), anti-Actin (Sigma, A2008, rabbit, 1:1000), anti-Tubulin (Sigma, T9026, mouse 1:1000) and anti-GAPDH (Sigma, G8705, mouse, 1:1000). After washing, the membrane was incubated with fluorescently-labeled secondary antibodies (IRDye 800CW Goat anti-Mouse, 926-32210; IRDye 680 Goat anti-Rabbit, 926-68071 LI-COR) and signals were recorded using the Odyssey Infrared Imaging system (LI-COR).

Northern Blot

Total RNA from cells was extracted as described above. Afterwards, polyA+ mRNA was enriched from total RNA using the Oligotex suspension (Qiagen) according to the manufacturer's instructions. 1.2 µg of polyA+ mRNA was glyoxylated and run on an agarose gel as described previously [4]. The RNA was transferred overnight using the Nytran SuPerCharge TurboBlotter system (Whatman) and UV-crosslinked.

DNA probes complementary to the *TP53* coding region or the 3′UTR were labeled with dCTP [α-^{32}P] using the Amersham Megaprime DNA labeling system (GE Healthcare). Primers used for

probe synthesis from human cDNA are listed in Table S2. Labeled probes were denatured by heat for 5 min at 90 °C and then incubated with the blot in ULTRAhyp Ultrasensitive Hybridization Buffer (Invitrogen) overnight at 42 °C. The blot was washed three times and exposed on a phosphorimaging screen. The radioactive signal was acquired using the Fujifilm FLA700 phosphorimager.

Human cell culture and drug treatment

Human cell cultures were maintained in a 5% CO_2/ 37 °C humidified environment. HEK293 cells were cultured in DMEM (high glucose) and HCT116 cells were cultured in McCoy's 5A medium which were supplemented with 10% FBS and 1% Penicillin/Streptomycin. Where indicated, HCT116 cells were treated with Etoposide (0.125-32 μM, Sigma), 5-fluorouracil (40 μM, Sigma), Nutlin-3 (20 μM, Seleckchem), or UV (50 J/m^2) prior to downstream analysis.

Reporter assays

We PCR-amplified the *TP53* 3′UTR sequence (nucleotides 1,380 to 2,586 of the reference mRNA NM_000546, May 2018) from WT HCT116 cDNA. This sequence was cloned downstream of the stop codon in pcDNA3.1-puro-eGFP using EcoRI/NotI restriction enzymes. For the dUTR construct, cDNA from TP53 dUTR HCT116 cells was used to amplify the remaining 3′UTR sequence after CRISPR-mediated deletion, representing a fusion of the first 12 and the last 157 nucleotides of the *TP53* 3′UTR. The p53 coding region, encoding the α protein isoform (1,182 nucleotides), was cloned upstream and in frame of the GFP-cassette using HindIII/BamHI restriction sites. For luciferase reporter studies, the full length 3′UTR and dUTR sequences described above were cloned into a SmaI-digested psiCHECK2 (Promega) vector via blunt-end cloning.

GFP reporter. GFP protein levels of cells transfected with equimolar amounts of GFP-containing reporter constructs was analyzed by flow cytometry after 24 hours. A BD LSRFortessa Flow Cytometer was used to record the mean fluorescence intensity (MFI) of 20,000 life cells. Raw data were analyzed using the FlowJo software package and values were normalized to GFP-only constructs. mRNA abundance of the GFP reporter was measured using RT-qPCR using the primers listed in Table S2. The GFP reporter mRNA was normalized to GAPDH mRNA.

Luciferase reporter assay. Luciferase activity was measured 24 hours after transfection of equimolar amounts of psiCHECK2 plasmids (Promega) containing either the *TP53* 3′UTR or dUTR sequence downstream of the Renilla luciferase translational stop codon. Cells were lysed in passive lysis buffer and Renilla and firefly luciferase activity was measured in duplicates using the Dual-Glo Luciferase Assay System (Promega) according to the manufacturer's instructions in a GloMax 96 Microplate Luminometer (Promega). Relative light units of Renilla luciferase were normalized to firefly luciferase activity.

Statistics and reproducibility

Statistical analysis of the mRNA and protein expression data was performed using a Student's t-test or ANOVA followed by a Tukey's multiple comparison test. We use ns ($p > 0.05$), * $0.01 < p < 0.05$, ** $0.001 < p < 0.01$ and *** $p < 0.001$ to indicate the levels of p-values in figures. The results for immunoblotting are representative of at least three biologically independent experiments. All statistical analyses and visualizations were performed by using GraphPad (Prism 8).

Online references

1 Behringer, R., Gertsenstein, M., Nagy, K., Nagy, A. *Manipulating the Mouse Embryo: A Laboratory Manual, Fourth Edition*. (CSH press, 2014).

2 Cong, L. *et al.* Multiplex genome engineering using CRISPR/Cas systems. *Science* **339**, 819-823 (2013).

3 Ran, F. A., Hsu, P. D., Wright, J., Agarwala, V., Scott, D. A. & Zhang, F. Genome engineering using the CRISPR-Cas9 system. *Nature protocols* **8**, 2281-2308 (2013).

4 Mayr, C. & Bartel, D. P. Widespread shortening of 3'UTRs by alternative cleavage and polyadenylation activates oncogenes in cancer cells. *Cell* **138**, 673-684 (2009).